



# Affinity capillary electrophoresis for identification of active drug candidates in myotonic dystrophy type 1

Ioan O. Neaga<sup>1,2</sup> · Stephanie Hambye<sup>1</sup> · Ede Bodoki<sup>2</sup> · Claudio Palmieri<sup>1</sup> · Eugénie Anseau<sup>3</sup> · Alexandra Belayew<sup>3</sup> · Radu Oprean<sup>2</sup> · Bertrand Blankert<sup>1</sup>

Received: 21 January 2018 / Revised: 16 March 2018 / Accepted: 24 April 2018 / Published online: 8 May 2018  
© Springer-Verlag GmbH Germany, part of Springer Nature 2018

## Abstract

Myotonic dystrophy type 1 (DM1) is an autosomal dominantly inherited degenerative disease with a slow progression. At the present, there is no commercially available treatment, but sustained effort is currently undertaken for the development of a promising lead compound. In the present paper we report the development of a fast, versatile, and cost-effective affinity capillary electrophoresis (ACE) method for the screening and identification of potential drug candidates targeting pathological ARN probes relevant for DM1. The affinity studies were conducted in physiologically relevant conditions using 50 mM HEPES buffer (pH 7.4) in a fused silica capillary dynamically coated with poly(ethylene oxide), by testing a library of potential ligands against (CUG)<sub>50</sub> RNA as target probe with a total run time of 4–5 h/ligand. For the most promising ligands, their affinity parameters were assessed and some results formerly reported on the affinity of pentamidine (PTMD) and neomycin against CUG repeats were confirmed. To the best of the authors' knowledge, the estimated binding stoichiometry for some of the tested compounds (i.e., ~ 121:1 for PTMD against the tested RNA probe) is reported for the first time. Additionally, the potential of a novel pentamidine like compound, namely 1,2-ethane bis-1-amino-4-benzamidine (EBAB) with much lower in vivo toxicity than its parent compound has also been confirmed studying its effect on a live cell model by fluorescence microscopy. Further tests, such as the evaluation of the rescue in the mis-splicing of the involved genes, can be performed to corroborate the potential therapeutic value of EBAB in DM1 treatment.

**Keywords** Myotonic dystrophy type 1 · Ligand screening · Affinity capillary electrophoresis · Fluorescence in situ hybridization · Pentamidine

## Introduction

Trinucleotides repeat expansions are mutations associated with several degenerative diseases including fragile X syndrome, spinocerebellar ataxia, Huntington's disease, and myotonic dystrophy types 1 and 2 [1, 2].

Myotonic dystrophy type 1 (DM1), also named Steinert's disease (OMIM #160900), is an autosomal dominantly inherited degenerative disease with a slow progression. It is one of the most common forms of adult-onset muscular dystrophy with a prevalence of about 1 in 20,000 [3–5], but in regions where there is a small variance in the gene pool, prevalence can rise up to 1 in 500 [6].

DM1 is a very complex condition that can alter many systems with a very wide interpatient variability. Muscles are affected, either by progressive weakness and loss of mass (dystrophy) or by difficulties to relax after contraction (myotonia). Other common symptoms include cataract, hypersomnia, fatigue, conductivity abnormalities, respiratory problems, and endocrinal dysfunctions [7, 8].

At genetic level, the disease is characterized by the expansion of cytosine-thymine-guanine (CTG) triplets in a non-coding region of the DMPK (dystrophin myotonia protein kinase) gene on chromosome 19, position 19q13.32 [9, 10]. Up to 35 triplet

✉ Bertrand Blankert  
bertrand.blankert@umons.ac.be

<sup>1</sup> Laboratory of Pharmaceutical Analysis, Faculty of Medicine and Pharmacy, Research Institute for Health Sciences and Technology, University of Mons, Place du Parc 20, 7000 Mons, Belgium

<sup>2</sup> Analytical Chemistry Department, "Iuliu Hațieganu" University of Medicine and Pharmacy, 4, Louis Pasteur St, 400349 Cluj-Napoca, Romania

<sup>3</sup> Laboratory of Molecular Biology, Faculty of Medicine and Pharmacy, Research Institute for Health Sciences and Technology, University of Mons, Place du Parc 20, 7000 Mons, Belgium

repeats is regarded as normal, whereas from 36 to 49 repeats it is considered a pre-mutation, the carriers being asymptomatic or very mildly affected. Nevertheless, the latter category of patients have an increased probability of transmitting more severe forms of the disease to their children because of genetic anticipation, i.e., increased triplet repeat expansion during transmission [11]. Above 50 CTGs repeats, the disease becomes clinically manifested. Generally, the higher the number of CTG repeats, the earlier and the more severe the disease will manifest [12–14].

The pathological mechanism is not completely elucidated yet, but it implies the  $(CTG)_n$  repeat expansion which is transcribed into toxic RNA with  $(CUG)_n$  repeats [15]. This RNA sequence will adopt a hairpin structure in the cell nucleus forming RNA *foci* able to sequester small molecules and proteins [2, 16]. Its toxicity can be attributed to the sequestration of splicing factors such as MBLN1 (Muscle Blind Like Protein 1) and CUGBP1, resulting in RNA mis-splicing and defective protein synthesis [15, 17].

For the moment, there is no available treatment for the disease, but several approaches are being investigated. Some of these include the following: suppressing the  $(CTG)_n$  repeat expansion in DNA [18], suppressing the toxic RNA and/or its structural hairpin [19], targeting the protein-RNA interactions by overexpressing the sequestered splicing factors [20, 21] and more recently, suppressing CTG repeats by CRISPR/Cas9 gene editing [22].

Currently most of the research is focused on targeting the RNA CUG repeats [18, 23–28]. For this purpose, small molecules and antisense nucleotides have been evaluated mainly by *in vitro* techniques. These molecules act either by disrupting the MBNL-1/CUG complex or by binding to abnormal CTG repeats in DNA, thus preventing its transcription into toxic RNA CUG triplets [18].

Warf et al. were the first to test small molecules with amino or guanidino moieties and for some of them reported a good affinity towards the  $(CUG)_n$  repeat expansion [29]. The main investigation tools employed were electrophoretic mobility shift assay (EMSA) and fluorescence microscopy, along with *in vivo* techniques to test a small library of RNA binding compounds. Two high affinity candidates were highlighted: pentamidine (PTMD), an antiprotozoal and antifungal drug, and neomycin B, an aminoglycoside antibiotic. Both were able to disrupt the MBNL1– $(CUG)_4$  complex, but only PTMD rescued the mis-splicing of the tested pre-mRNAs. However, the elevated concentrations of PTMD required for a noticeable *in vivo* effect are associated with cellular toxicity [29] thus hindering its clinical applicability. Nevertheless, their work paved the way for further study on other small molecules able to fight DM1 and over the last decade several other promising ligands were reported [23, 28, 30–33].

*In vitro* methods for affinity studies are mainly EMSA and fluorescence microscopy, but the difficulty of their automation hinders the screening of large libraries of compounds.

Capillary electrophoresis (CE) has been successfully used for the study of the binding process in various types of interactions [34–46]. Several CE techniques are routinely used in the investigation of bio-interactions, but very rarely for the study of nucleic acid-ligand interaction [47].

Affinity capillary electrophoresis (ACE) is an electrophoretic technique developed in the 1990s, initially being used for the study of protein-ligand interactions [48–50]. In certain aspects, ACE is similar to affinity chromatography. One of the tested molecules, arbitrarily named ligand, is added to the running buffer and the other, the analyte, is to be injected as a sample. The ligand in the buffer will constitute a pseudo-stationary phase, and upon its dynamic interaction with the analyte, it will decrease the electrophoretic mobility of the latter. The binding constant can be estimated based on the changes recorded in the analyte's migration time (and electrophoretic mobility) as a function of ligand concentration. ACE is a fairly simple and straightforward analytical technique suitable for the investigation of both weak and strong interactions, but several prerequisites must be met for its use. First, the analyte and its complex with the ligand must present distinct migration times and second, the time range required for the interaction to reach a dynamic equilibrium must be lower than the separation time. As a consequence, the ligand concentration should ideally be at least 1 order of magnitude higher than that of the analyte [51]. Nevertheless, working in equilibrium conditions imply good estimates of the binding constants.

ACE presents several advantages over the conventional methods of determining binding constant (i.e., liquid chromatography, competition dialysis) as well as over other CE techniques [51]. Compared to HPLC, exclusion chromatography, or competition dialysis, ACE requires much smaller volumes of both ligand and analyte, significantly reducing costs when one of the molecules is expensive or is of limited accessibility. Furthermore, its high separation efficiency enables the assessment of binding constants also for analytes with lower purity. The possibility of ACE automation is another valuable asset for the screening of large libraries of compounds [47, 51, 52].

Some of the ACE drawbacks are linked to the intrinsic CE characteristics. Biomolecules may interact with the inner wall of the silica capillary, leading to poor performance and biased estimations of the binding parameters. Fortunately, capillary coating (permanent or dynamic) can suppress both wall interactions and potentially undesirable electroosmotic flow (EOF). As in case of all CE techniques using UV-VIS detection, ACE presents higher detection limits compared to high-performance liquid chromatographic techniques [53] due to the very short optical pathway.

Despite its compelling advantages, to this date CE has not been exploited for the screening of ligands with potential use in DM1 treatment. In the present study, the performance of ACE for the screening of plausible ligands for RNA (CUG) repeats is demonstrated. Particularities of method

development and further improvements of the screening protocol and data analysis are also proposed. The proposed screening method highlighted a novel ligand for CUG repeats, namely 1,2-ethane bis-1-amino-4-benzamidine (EBAB), and a first biological evaluation in a cell model using fluorescence microscopy was used to confirm the results.

## Materials and methods

### Reagents

All used chemicals were of analytical grade or higher and were purchased from different suppliers: HEPES (4-(2-hydroxyethyl)-1-piperazineethanesulfonic acid), polyethylene oxide (PEO) 200K, PTMD isethionate, and imidazole were acquired from Sigma-Aldrich (St. Louis, MO, USA). Bacitracin, chloramphenicol, neomycin, clindamycin, tetracycline, doxycycline, oxytetracycline, erythromycin, xylometazoline, naphazoline, and metformin were purchased from ACA Pharma (Nazareth, Belgium). EBAB (a PTMD analogue) was synthesized as described in the literature [54, 55]. The RNA probe with 50 CUG repeats was synthesized by Bio-Synthesis Inc. (Lewisville, TX, USA).

Ultrapure deionized water (18.2 M $\Omega$ ) was used for the preparation of all the working solutions and buffers (Milli-Q $\text{\textcircled{R}}$  Reference Water Purification System, Merck, USA).

A 50 mM HEPES (pH = 7.4) buffer solution (kept at  $-4\text{ }^{\circ}\text{C}$ ) was used for the dissolution of the ligands. A ligand stock solution ( $\sim 1\text{ mM}$ ) kept at  $-20\text{ }^{\circ}\text{C}$  served for the preparation of daily fresh aliquots in HEPES buffer. All working solutions were passed through 0.2  $\mu\text{m}$  pore size Spartan syringe filters (Whatman, Little Chalfont, UK) and degassed by sonication for at least 5 min before use.

For the dynamic coating of the bare fused silica capillary, a PEO coating solution was employed according to the protocol described by Tran et al. [30]. A stock solution, being stable for at least a week [56], was prepared by dissolving in ultrapure water 22.2 mg of PEO under stirring at 40–50  $^{\circ}\text{C}$ . The PEO coating solution was prepared each day by mixing 1 M HCl with PEO stock solution in 1:9 ratio, passing the resulting solution (0.2 g PEO/mL 0.1 M HCl) through a 0.8- $\mu\text{m}$  pore size, 25 mm Whatman $\text{\textcircled{R}}$  SPARTAN syringe filter (Whatman, Little Chalfont, UK).

Marvin Suite v. 16 (ChemAxon, Budapest, Hungary) was used to assess the main ionic form of the ligands at pH 7.4.

### Capillary electrophoresis

The experiments were performed using an Agilent G1600 capillary electrophoresis system (Agilent Technologies, Germany) and the samples were injected hydrodynamically (50 mbar  $\times$  5 s).

The bare fused silica capillary was acquired from Polymicro Technologies, USA. Polyvinyl alcohol-coated (PVA) and fluorocarbon-coated (FC) capillaries were purchased from Agilent Technologies, USA, whereas the linear polyacrylamide (LPA)-coated capillary was obtained from Beckman Coulter, USA. All capillaries had an internal diameter of 50  $\mu\text{m}$ , an external diameter of 365  $\mu\text{m}$ , and total length of 40 cm. Detection was performed with the built-in diode-array detector, recording the signals at three different wavelengths: 230, 260, and 280 nm.

The PEO-coated capillary was prepared according to a modified version of Tran et al. protocol and involved several steps [56]. Briefly, the bare fused silica capillary was first conditioned by washing sequentially for 5 min each with ultrapure water, 1 M NaOH, 0.1 M NaOH, and again with ultrapure water. The first coating was done by rinsing the capillary for 5 min each with ultrapure water and 1 M NaOH, followed by 10 min each with 1 M HCl and ultrapure water and finally for 5 min each with PEO coating solution (0.20 g/100 mL in 0.1 M HCl) and water. At the beginning of each day, the capillary coating was regenerated by washing for 2 min with ultrapure water, 5 min each with 1 M HCl and PEO coating solution, and 2 min with the background electrolyte. Between each analysis, the capillary was conditioned by rinsing for 3 min each with ultrapure water and 1 M HCl solution, followed by another 5 min with PEO coating solution, and finally a 2-min wash with the working buffer.

### Affinity capillary electrophoresis and the assessment of binding constant

A fused silica capillary coated with PEO as described in section “Capillary electrophoresis” was used for the ACE experiments ( $L_t = 40\text{ cm}$ ,  $L_{eff} = 31.5\text{ cm}$ ). The (CUG)<sub>50</sub> RNA (5  $\mu\text{M}$ ) sample was hydrodynamically injected (50 mbar  $\times$  5 s) at the long end of the capillary. The (CUG)<sub>50</sub> RNA sample was first ran in plain buffer (50 mM HEPES, pH 7.4) and subsequently in 50 mM HEPES buffer with increasing concentrations (from 0 up to 100  $\mu\text{M}$ ) of the tested ligand. The analyses were performed in triplicate ( $n = 3$ ) at a separation voltage of  $-15\text{ kV}$  and the detection was done at the characteristic UV absorption maxima of the RNA probe (260 nm). Each ACE assay lasted for 14 min with a total run time of 31 min (including the preconditioning step).

At each level of ligand concentration, the analyte’s electrophoretic mobility was calculated based on its recorded migration time using the following formula (1):

$$\mu = L_t \times L_{eff} / (t_m \times V) \quad (1)$$

where  $L_t$  is the total capillary length,  $L_{eff}$  is the effective capillary length (the length up to the detector),  $t_m$  is the analyte’s migration time, and  $V$  is the separation voltage.

The binding constant for each ligand was assessed using two different methods, based on a linear and a nonlinear regression. The Scatchard method for ACE is a linear approach based on the original method used to determine the binding constants between proteins and ligands [57], using the following adapted equation:

$$\Delta\mu/L = K_b \times \Delta\mu_{max} - \Delta\mu \times K_b \quad (2)$$

where  $\Delta\mu$  is the difference in the electrophoretic mobility for the analyte with either no ligand or a given ligand concentration in the buffer,  $L$  is the ligand's concentration in the buffer,  $K_b$  is the binding constant, and  $\Delta\mu_{max}$  is the maximum difference in electrophoretic mobility (in the absence and presence of the ligand in the buffer).

By the nonlinear regression approach, data fitting is based on a slightly more complex equation [58] (3):

$$\Delta\mu = K_b \times (\mu_{max} - \mu_0) \times [L / (1 + K_b \times L)] \quad (3)$$

In this case, known terms carry the same meaning as in Eq. (2), whereas  $\mu_0$  is the electrophoretic mobility of the analyte with no ligand in the buffer and  $\mu_{max}$  is the mobility of the analyte at the maximum concentration of ligand, above which there is no more change in the mobility.

For basic data analysis and linear regression using the Scatchard method, the Excel software was used (Microsoft Office 2016 Package), whereas for nonlinear regression Origin 2016 (OriginLab, trial version) was employed.

### Capillary zone electrophoresis for stoichiometry determination

Method parameters were almost identical with the ones used for ACE using PEO-coated fused silica capillary ( $L_t = 40$  cm,  $L_{eff} = 31.5$  cm), 50 mM HEPES buffer (pH 7.4) as running buffer, and a separation voltage of +15 kV. For these experiments, a high concentration of ligand (700–900  $\mu$ M) previously shown by ACE to interact with the RNA sample (analyte) was used. The high ligand excess was meant both to fully saturate the analyte and to assure a sufficient amount of free ligand for accurate detection and quantification.

A plug of RNA (CUG)<sub>50</sub> 5  $\mu$ M was first injected (50 mbar  $\times$  5 s) followed by an identical plug of the ligand (700–900  $\mu$ M). Upon applying a positive separation voltage (no incubation time), the positively charged ligand (pH 7.4) migrated in an opposite direction with the negatively charged RNA sample. The two plugs passing through each other may interact forming a complex while the excess free ligand was detected at the cathode.

## Fluorescence microscopy

### Biological material

pMBNL1-GFP and pDT960 minigene plasmids were kindly provided by Denis Furling (Institute of Myology, Paris, France) and Thomas Cooper (Baylor College of Medicine, Houston, USA). DT960 vector contained 960 interrupted CTG repeats. GFP-tagged MBNL1 protein is expressed from pMBNL1-GFP vector. PTMD and EBAB (see section "Reagents".) were prepared in RNase free water (1 mg/mL). DMSO was added to enhance the analogue's solubility (highest concentration in DMSO, 8%).

### Cell culture and transfection

The protocol was slightly adapted from [29]. HeLa, a cervix adenocarcinoma cell line, were obtained from ATCC® (Number CCL-2). Cells were cultured in DMEM-F12 growth medium (Lonza, Belgium) supplemented with 10% FBS (Fetal Bovine Serum Gold, PAA Laboratories, Toronto, Canada). Cells ( $3 \times 10^5$ ) were seeded in six-well plates onto coverslips and were transfected 24 h later with 1  $\mu$ g pGFP-MBNL1 and 750 ng pDT960 plasmids per plate using Lipofectamine 2000 (Invitrogen, Carlsbad, CA, USA) according to the manufacturer's protocol. After transfection, PTMD (50, 75, and 100  $\mu$ M), EBAB (50, 75, and 100  $\mu$ M), or water (control) were added to the cell culture medium and the cells were fixed 20 h later. Each experiment was performed in triplicate. Cells were fixed for 10 min at 4 °C and 5 min at room temperature (RT) with 4% paraformaldehyde and then washed three times with 1 $\times$  phosphate borate saline (PBS) and once with ultrapure water.

### FISH

For the fluorescence in situ hybridization (FISH) procedure, cells were permeabilized with 0.5% Triton X-100, in 1 $\times$  PBS at RT for 5 min. Cells were prewashed with 30% formamide, 2 $\times$  SSC at RT for 10 min before hybridization for 2 h at 37 °C with 1 ng/mL of Atto 594 2-O-methyl(CAG)<sub>20</sub> fluorescent probe (Eurogentec, Liège, Belgium) in 30% formamide, 2 $\times$  SSC (sodium chloride 3 M/sodium citrate buffer 0.3 M), 2  $\mu$ g/mL BSA, 66  $\mu$ g/mL yeast tRNA, and 2 mM vanadyl complex. Cells were then washed for 30 min at 42 °C with 30% formamide, 2 $\times$  SSC and 30 min at RT in 1 $\times$  SSC and then mounted onto glass slides using the hard-set mounting media that contains 4,6-diamidino-2-phenylindole (DAPI; SlowFade® Gold Antifade, Life Technologies). Cells were imaged on a Nikon Eclipse 80i microscope with DS-U3 camera and NIS Elements-BR software.

## Statistical analysis

The effectiveness of compound binding was evaluated after scoring the number of nuclei presenting foci and, if present, the number of *foci* per nucleus ( $\leq 2$ ,  $\leq 5$ , or  $> 5$ ). Ten fields were analyzed per assay. Statistical analyses were performed with GraphPad Prism 5 software (GraphPad Software, La Jolla, USA). One-way ANOVA with post hoc Student's *t* tests (Dunnet correction) was used to evaluate whether the decrease of the percentage of *foci* per nucleus was significant compared to the control. Two-way ANOVA with post hoc Student's *t* tests (Bonferroni correction) was used to compare the populations of nuclei classified according to the number of foci they contain ( $\leq 2$ ,  $\leq 5$ , or  $> 5$ ) in cells treated or not with the drug. *p* values  $< 0.05$  were considered significant.

## Results and discussions

### PTMD as a model ligand to set up ACE conditions

The buffer's pH, which can influence the nucleic acid and ligand's charge and therefore their mutual interaction, is an important factor in affinity studies. Since the simulation of nucleic acid-ligand interactions are of interest in physiologically relevant conditions, 50 mM HEPES buffer at pH 7.4 was used throughout all CE experiments. HEPES, besides its good buffering capacity at physiological pH, was chosen over other buffering systems (i.e., phosphate) by providing better solubility for PTMD and EBAB.

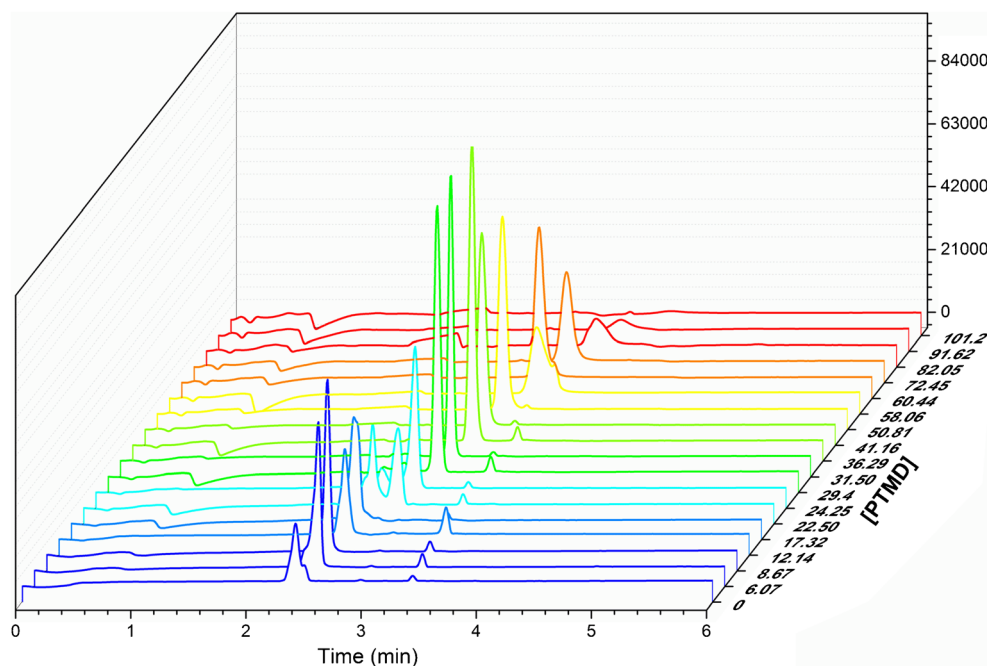
To reduce the adsorption of PTMD and other biomolecules onto the inner capillary wall (which can lead to reproducibility

and recovery problems), as well as to decrease the EOF, several permanently or dynamically coated capillaries were evaluated for our experiments. The actual values of the electroosmotic mobility were assessed for commercially available capillaries with covalent coating and for a bare fused silica capillary dynamically coated with PEO. The PEO-coated capillary was selected for further experiments, demonstrating the highest efficiency in EOF suppression while also being the most cost-effective option. As a direct consequence of the EOF suppression, the lowest variability in RNA (CUG)<sub>50</sub> migration times (0.25 RSD% intra-day and 0.53 RSD% inter-day, respectively) was also recorded using this PEO-coated capillary.

As mentioned earlier, ACE is quite simple and requires a reduced number of operational steps. First, the electrophoretic mobility of the analyte ((CUG)<sub>50</sub> RNA) is measured running the assay in an appropriate buffer system as background electrolyte. In the next steps, sequential assays are conducted to follow the changes in the analyte's electrophoretic mobility in the presence of increasing ligand (PTMD) concentrations dissolved in the running buffer.

The RNA migration time increased with the PTMD concentration in the running buffer, whereas no RNA peak could be detected above 100  $\mu$ M PTMD (Fig. 1). Besides the observed changes in the electrophoretic mobility of the (CUG)<sub>50</sub> RNA, variations of the peak height and area were noticed showing a bimodal pattern as a function of PTMD concentration, with a maximum around 9 and 50  $\mu$ M. It can be hypothesized that  $\pi$ - $\pi$  type interactions between PTMD molecules and the RNA may be potentially associated with conformational changes, leading to changes of the transient (CUG)<sub>50</sub>-PTMD complex's molar absorptivity, considering that both

**Fig. 1** ACE assays of the (CUG)<sub>50</sub> RNA fragment at increasing PTMD concentrations. Conditions: 50 mM HEPES buffer, pH = 7.4; RNA plug 50 mbar  $\times$  5 s. Fused silica capillary dynamically coated with PEO,  $L_{\text{tot}}$  = 40 cm,  $L_{\text{eff}}$  = 31.5 cm, -15 kV



the RNA and PTMD have their maximum absorption at 260 nm. Intriguingly, this phenomenon was not observed with the other tested ligands. Another observed phenomenon was a peak splitting at 24.25 and 29.4  $\mu\text{M}$  PTMD, potentially associated with the transition of the  $(\text{CUG})_{50}$ -PTMD complex between the two conformational states. In this case, the average migration time of the two peaks has been employed during the data fitting procedure. Nevertheless, further studies are required for a better understanding of  $(\text{CUG})_{50}$ -PTMD interaction mechanism.

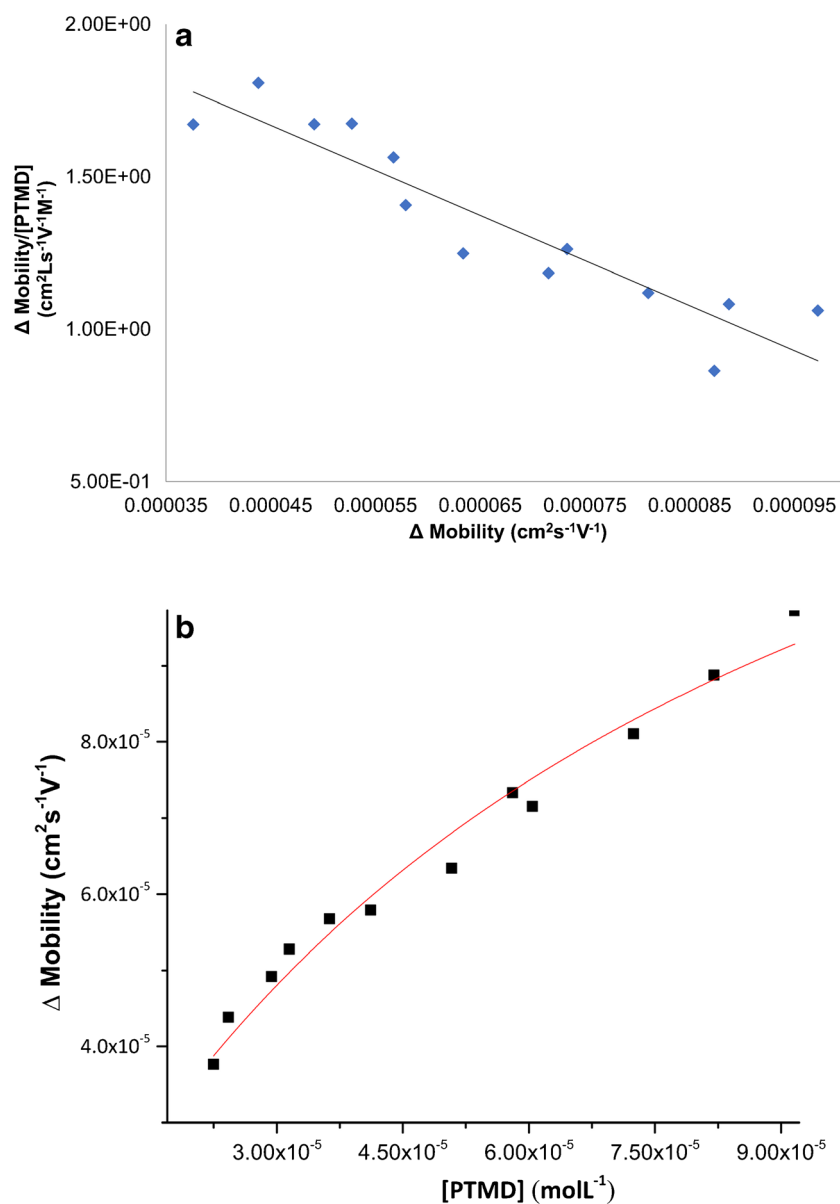
Additionally, at higher PTMD concentrations, changes in the complex's peak profile may also be distinguished, the peaks becoming smaller and wider. As RNA and PTMD carry opposite charges at this pH and due to the rising concentration of ligand in the buffer, the RNA charge will progressively be

neutralized, leading to an elongated peak that disappears above 100  $\mu\text{M}$  PTMD.

Generally, in affinity studies, data fitting may be accomplished by several means [59, 60], out of which two of the most popular approaches for ACE were tested: a modified version of Scatchard analysis and a nonlinear data fitting. The Scatchard method (Fig. 2a) involves a linear regression, where the negative value of the slope ( $Y = -14,788X + 2.3341$ ,  $R^2 = 0.860$ ) is the estimated binding constant ( $K_b = 14.79 \times 10^3 \text{ M}^{-1}$ ).

Scatchard analysis was one of the first methods used for data extraction in ACE [48–50]. It presents several disadvantages linked to the use of dependent variables on both  $x$  and  $y$  axes, generating sometimes inexistent correlation [57] and increasing the risk of overlooking low-affinity binding components [61].

**Fig. 2** Data fitting for the interaction between PTMD and  $(\text{CUG})_{50}$  RNA probe. **a** Fitting using Scatchard method **b** Fitting using nonlinear regression



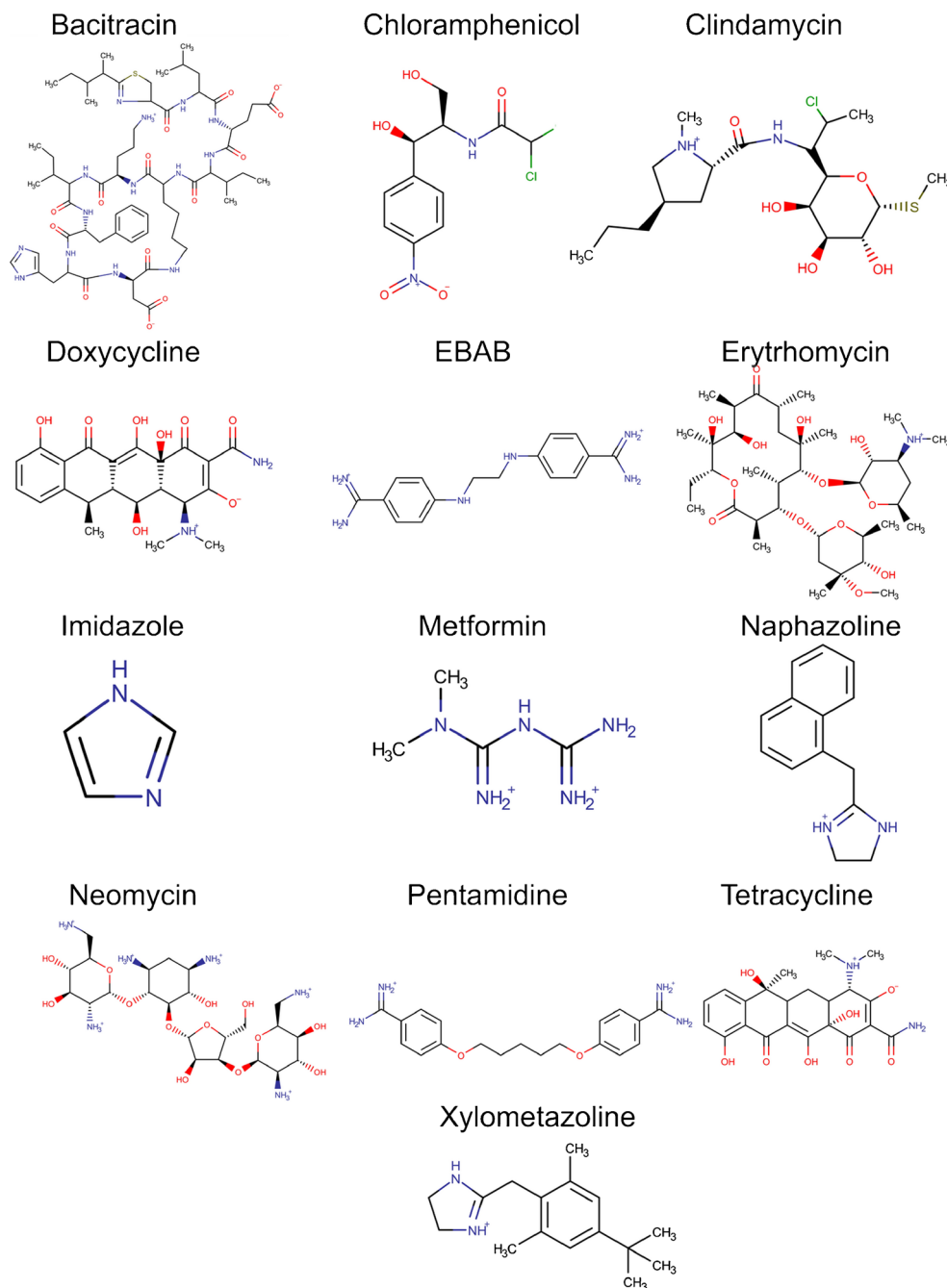
Despite these drawbacks, this approach is still currently used in ACE due its simplicity, while also providing means of detecting more than one type of interaction. For instance, biomolecules will generate on the same regression line distinct slopes for each non-equivalent binding site [62].

Nonlinear regression methods are considered better for data extraction in terms of accuracy and precision compared to linear regression [60, 63, 64]. By using nonlinear fitting of the electrophoretic data for PTMD (Fig. 2b,  $R^2 = 0.970$ ), the estimated binding constant is  $K_b = 13.11 \times 10^3 \text{ M}^{-1}$ . Both methods gave similar results in terms of PTMD binding constant ( $K_b =$

$14.79 \times 10^3 \text{ M}^{-1}$  for the Scatchard method and  $K_b = 13.11 \times 10^3 \text{ M}^{-1}$  for the nonlinear data fitting method).

During ACE method, development of high importance was the finding of an adequate internal standard. The ideal ACE internal standard, apart of being stable under the experimental conditions, should not interact in any way with the analyte nor the ligand and preferably it should have a lower migration time than the analyte. Several molecules with electrophoretic behavior similar to the analyte ((CUG)<sub>50</sub> RNA) were considered, such as AMP, ADP, ATP, benzoic acid, and pyromellitic acid (data not shown). ATP provided shorter and more

**Fig. 3** Ligands tested by ACE. If applicable, the major charged species of the ligands existing at pH 7.4 were represented (as simulated in Marvin Suite v. 16, ChemAxon)



reproducible migration times (RSD% < 0.8) compared to (CUG)<sub>50</sub> RNA, but its relatively fast hydrolytic degradation rendered it of limited practical use. Pyromellitic acid, in spite of its good stability and favorable electrophoretic behavior, showed signs of interaction with some of the ligands, the strongest in case of neomycin. Due to these constraints, the ACE method developed for the screening of potential drug candidates in DM1 was further optimized without the use of an internal standard.

## Screening of a small library of ligands

### Selection of the library

As a next step, several other ligands were chosen to be tested using the same protocol. These ligands (Fig. 3) were selected either based on their structure, looking for nitrogen-rich functionalities (amine, guanidine, carboximidamide or N-based heterocycles), or based on previous proofs of interaction with the CUG motifs [18, 21, 29].

A special attention was allocated to EBAB, a PTMD analogue, with a much lower toxicity than its parent compound, which was initially synthesized as an antiparasitic compound [54]. In vitro and in vivo studies also acknowledge it as promising drug candidate for the treatment of *Pneumocystis carinii* pneumonia [54, 55]. Additionally, EBAB has also demonstrated antioxidant, neuroprotective, and anticonvulsant properties [65], for which pharmacokinetic studies have already been performed using a rat model [66, 67].

### Ligand screening test

A high throughput screening test based on a simplified ACE protocol was set up to select potential candidates for further affinity studies. Each ligand was screened at a single high concentration (~ 1 mM) using the same electrophoretic conditions described in section “Affinity capillary electrophoresis and the assessment of binding constant,” looking for changes in the (CUG)<sub>50</sub> RNA probe migration time in comparison with the ligand-free control assay (Fig. 4).

For most ligands, no change in the electrophoretic mobility of the nucleic acid probe has been recorded except for neomycin and EBAB, for which the (CUG)<sub>50</sub> RNA peak completely disappeared, suggesting a possible interaction. Based on these initial screening results, neomycin and EBAB were subjected to the full affinity protocol described in sections “Affinity capillary electrophoresis and the assessment of binding constant” and “PTMD as a model ligand to set up ACE conditions.”

### Estimation of the binding constant for selected ligands

Following the screening test, neomycin and EBAB were evaluated according to the full procedure described for PTMD. The binding constant estimates, using linear and nonlinear regressions, are synthesized in Table 1. As it can be seen, the ligands demonstrating the highest affinity towards (CUG)<sub>50</sub> RNA are neomycin, followed by PTMD and EBAB.

Our estimated (CUG)<sub>50</sub> RNA binding constants of PTMD and neomycin seem to be consistent with the ones

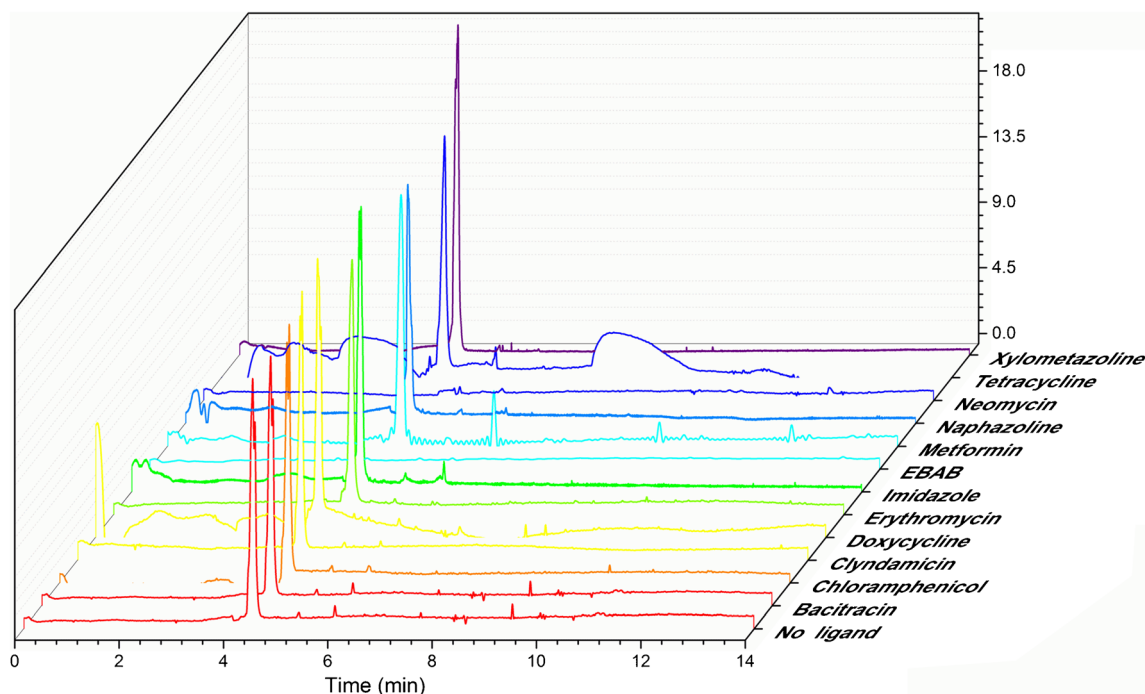


Fig. 4 Screening of ligands (~ 1 mM in the running buffer) with the (CUG)<sub>50</sub> RNA probe



**Table 1** Estimated binding constants for ligands demonstrating affinity towards (CUG)<sub>50</sub>

Estimated binding constants	Estimated binding constants	
	Nonlinear regression	Scatchard analysis
PTMD	$13.11 \times 10^3 \text{ M}^{-1}$	$14.78 \times 10^3 \text{ M}^{-1}$
EBAB	$10.17 \times 10^3 \text{ M}^{-1}$	$12.09 \times 10^3 \text{ M}^{-1}$
Neomycin	$59.18 \times 10^3 \text{ M}^{-1}$	$56.16 \times 10^3 \text{ M}^{-1}$

previously reporting a high affinity between these ligands and a (CUG)<sub>4</sub> RNA probe [29]. In the said study, EMSA was used to determine the IC<sub>50</sub> of the ligands disrupting the CUG-MBNL1 complex. The reported values of IC<sub>50</sub> for PTMD ( $58 \pm 5 \mu\text{M}$ ) and for neomycin ( $280 \pm 40 \mu\text{M}$ ) apparently indicate a higher binding affinity for PTMD, being more efficient in disrupting the CUG-MBNL1 complex [29]. The reversal of the affinity ranking between neomycin and PTMD in the two different studies could be attributed to the differences in length of the studied CUG repeats (50 vs. 4 CUG repeats). Furthermore, a putative difference in the interaction mechanism between these two ligands and the preformed CUG-MBNL1 complex compared to the free RNA may also be held responsible. Further ACE studies implying the use of (CUG)<sub>n</sub>-MBNL1 complex as analyte could clarify the above hypothesis.

Nevertheless, since neomycin does not save the mis-splicing of the affected genes [29], EBAB becomes the prime candidate for further *in vivo* studies in the DM1 context, since it is a less toxic analog of PTMD, demonstrating good cellular tolerance.

## Estimation of the interaction stoichiometry

Since the determination of interaction stoichiometry between the ligand and the CUG-repeat RNA could provide further useful information, such as the number of binding sites on the (CUG)<sub>50</sub> RNA molecule and the binding efficiency of the ligand, a simple CE method, complimentary to the ACE, was further proposed (section “[Capillary zone electrophoresis for stoichiometry determination](#)”).

The stoichiometry of (CUG)<sub>50</sub> RNA probe interaction with PTMD and EBAB has been investigated, building as a first step the calibration curves using linear regression of peak area versus nominal concentration of the pure ligand in the range of 50–1000  $\mu\text{M}$  for both PTMD and EBAB.

Based on the obtained regression equations ( $y = 0.1889x - 1.5345$ ,  $r^2 = 0.9985$  for PTMD, and  $y = 0.2635x - 8.0881$ ,  $r^2 = 0.9971$  for EBAB, respectively), the amount of free ligand reaching the detector has been assessed. By knowing the total amount of injected ligand enabled the estimation of the amount of ligand bound to the RNA probe ((CUG)<sub>50</sub>) and the average interaction stoichiometry ( $120.92 \pm 6.08$  for PTMD, and  $122.99 \pm 2.51$  for EBAB, respectively). It can be observed that both PTMD and its analogue, EBAB, exhibit similar stoichiometry in the interaction with the (CUG)<sub>50</sub> RNA probe.

A simple and straightforward estimation of the binding stoichiometry is very important, because the global efficiency of a potential drug candidate could be determined not only from its affinity for the RNA probe, but also from the number of molecules of ligand needed to inactivate the targeted molecule of RNA. For example, if a certain molecule has a high affinity and low stoichiometry towards the CUG motif, that would mean that the said molecule would require a lower dose *in vivo*.

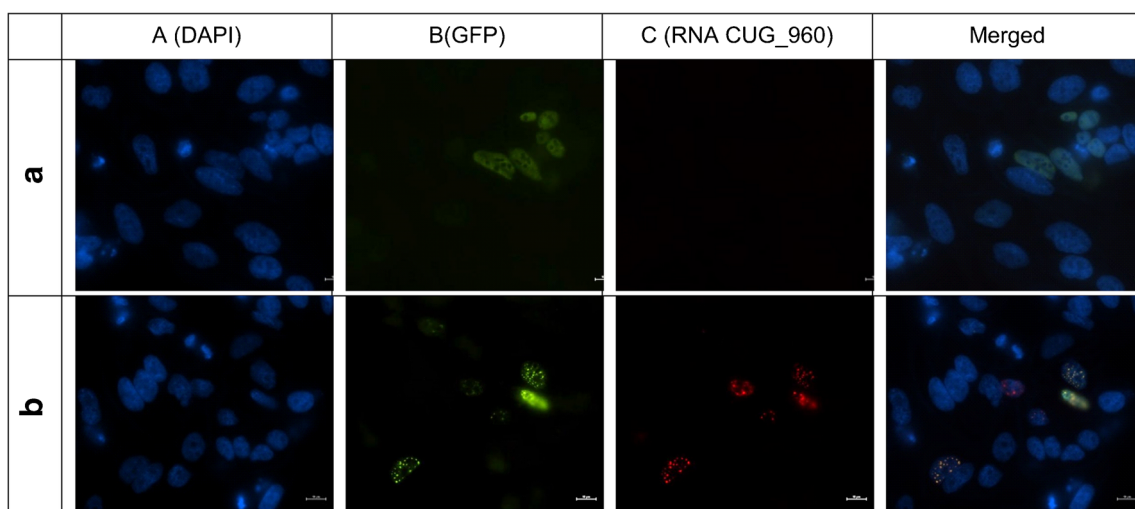


**Fig. 5** **a** Transfection of HeLa cells with pMBNL1-GFP plasmid alone. Fluorescence microscopy showed MBNL1-GFP protein (GFP, green) localized to the nucleoplasm. **b** Co-transfection of HeLa cells with pDT960 and pMBNL1-GFP plasmids. A characteristic DM1 pattern

was observed where MBNL1-GFP (green) co-localized in nuclear foci with the CUG repeat RNA detected by fluorescent *in situ* hybridization (RNA CUG<sub>960</sub>, red). Nuclei were stained with DAPI (blue). Scale, 10  $\mu\text{m}$ . For details, see Method section

**Table 2** Change in the abundance of nuclei presenting *foci* and the number of *foci* per nucleus after PTMD or EBAB treatment

	Concentration ( $\mu\text{M}$ )	Percentage of nuclei presenting <i>foci</i> ( $\bar{x} \pm \delta$ )	Decrease (%)	Percentage of nuclei presenting <i>foci</i> ( $\bar{x} \pm \delta$ ), classified in three populations depending on the number of <i>foci</i> per nucleus		
				$\leq 2$	$\leq 5$	$> 5$
[PTMD]	0 $\mu\text{M}$ (control)	83.0 $\pm$ 14.0		23 $\pm$ 6	16.0 $\pm$ 3.0	44.0 $\pm$ 10.0
	50 $\mu\text{M}$	54.0 $\pm$ 8.0	29.0 (*)	18.0 $\pm$ 13.0 (n.s.)	19.0 $\pm$ 2.0 (n.s.)	17.0 $\pm$ 6.0 (*)
	75 $\mu\text{M}$	44.0 $\pm$ 9.0	39.0 (**)	16.0 $\pm$ 13.0 (n.s.)	10.0 $\pm$ 7.0 (n.s.)	18.0 $\pm$ 9.0 (*)
	100 $\mu\text{M}$	41.4 $\pm$ 0.8	41.6 (**)	19.0 $\pm$ 21.0 (n.s.)	15.0 $\pm$ 16.0 (n.s.)	8.0 $\pm$ 6.0 (***)
[EBAB]	0 $\mu\text{M}$ (control)	85.0 $\pm$ 4.0		23.0 $\pm$ 3.0	26.0 $\pm$ 5.0	36.0 $\pm$ 3.0
	50 $\mu\text{M}$	62.0 $\pm$ 5.0	23.0 (***)	22.0 $\pm$ 4.0 (n.s.)	16.0 $\pm$ 3.0 (n.s.)	24.0 $\pm$ 4.0 (*)
	75 $\mu\text{M}$	54.0 $\pm$ 4.0	31.0 (***)	17.0 $\pm$ 6.0 (n.s.)	13.0 $\pm$ 5.0 (*)	24.0 $\pm$ 10.0 (*)
	100 $\mu\text{M}$	42.0 $\pm$ 4.0	43.0 (***)	17.0 $\pm$ 2.0 (n.s.)	11.0 $\pm$ 4.0 (**)	14.0 $\pm$ 6.0 (***)

HeLa cells were co-transfected with pDT960 and pMBNL1-GFP plasmids (see Methods). PTMD or EBAB (50, 75, and 100  $\mu\text{M}$ ) were added to the culture medium and cells grown for a further 20 h. MBNL1-GFP (green) was observed under a fluorescence microscope and localized in nuclear foci as it was sequestered by CUG-repeat RNA as shown in Fig. 6B. Nuclei and *foci* were counted on 10 microscope fields of three replica plates. In the last columns, the nuclei presenting *foci* were grouped into three subsets ( $\leq 2$  *foci*,  $\leq 5$  *foci*,  $> 5$  *foci*). The averages are presented with standard deviation and statistical significance is presented with  $p < 0.05$  (\*),  $p < 0.01$  (\*\*), or  $p < 0.001$  (\*\*\*)

Our current ongoing research using a more representative disease probe with higher number of CUG repeats ( $> 50$  CUG) and the inclusion of the MBNL-1 protein in the study protocol will remain to confirm the above hypothesis.

## Fluorescence microscopy

To further investigate the therapeutic potential of EBAB in DM1, a biological evaluation by fluorescence microscopy in a cell model was performed for the first time. A slightly adapted version of a previously published protocol (see section “Cell culture and transfection”) was employed, in which HeLa cells were transfected with two plasmids. The first one, pMBNL1-GFP, encodes GFP-tagged MBNL-1 protein and allows its visual localization in the nucleus. The second plasmid, pDT960, is transcribed into a CUG repeat RNA which is detected by FISH procedure using a specific fluorescent RNA probe. The co-transfected cells present a classic DM1 pattern with characteristic nuclear RNA *foci* that colocalize with the MBNL-1 protein due to its sequestration by CUG repeat hairpins (Fig. 5b (A–D)). In contrast, a non-pathological pattern, where MBNL1 localizes to the nucleoplasm of cells, is observed upon transfection with pMBNL1-GFP vector alone (Fig. 5a (A–D)).

Since PTMD was previously highlighted as an active compound, it was used as a positive control to evaluate EBAB activity and toxicity in co-transfected HeLa cells. PTMD or EBAB were added to the culture medium at three different concentrations. Treatment response was evaluated 20 h later under fluorescence microscopy by counting the number of nuclei presenting RNA *foci* that were visualized in green

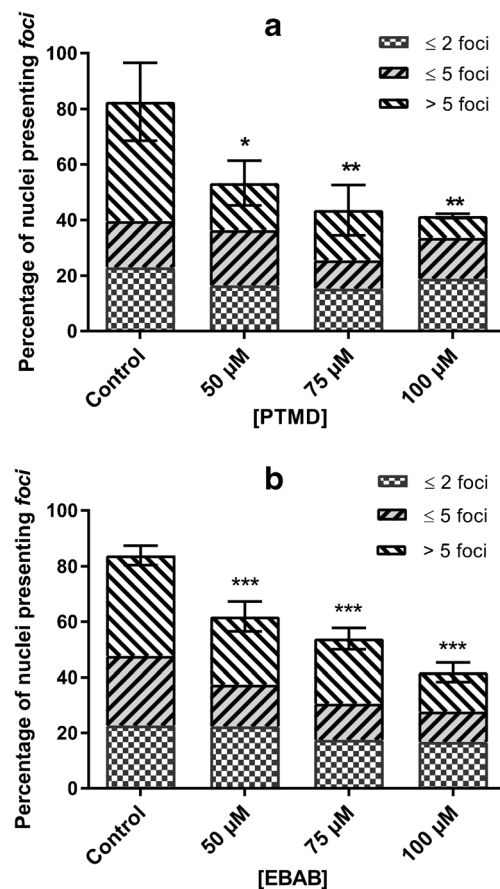


**Fig. 6** Percentage of nuclei presenting *foci* and number of *foci* per nucleus after addition of PTMD (A) or EBAB (B) (50, 75, or 100  $\mu\text{M}$ ) as described in Table 2. Nuclei presenting *foci* are subdivided into three subsets ( $\leq 2$  *foci*,  $\leq 5$  *foci*,  $> 5$  *foci*). Statistically significant with  $p < 0.05$  (\*),  $p < 0.01$  (\*\*), or  $p < 0.001$  (\*\*\*)

because they sequestered MBNL1-GFP. These nuclei were classified into three distinct populations according to the number of *foci* they presented. The data are presented in Table 2 and Fig. 6.

Upon the addition of 75  $\mu\text{M}$  PTMD or EBAB, the formation of nuclear *foci* was reduced by 39% ( $p < 0.01$ ) and 31% ( $p < 0.001$ ), respectively. At a 100  $\mu\text{M}$  concentration, the decrease of nuclear *foci* was even more pronounced, arriving to 41.6% ( $p < 0.001$ ) and 43% ( $p < 0.001$ ) for PTMD and EBAB, respectively. A decrease in numbers of *foci* was previously described upon PTMD addition [29]. As observed in previous and in the current study, a huge cell mortality after addition of 100  $\mu\text{M}$  PTMD was experienced, confirming its high toxicity. However, this was not the case after the addition of 100  $\mu\text{M}$  EBAB, as anticipated from its lower toxicity [54].

Cellular studies combined with ACE data endorse EBAB as an active binder to CUG-repeat RNA probes, while having a much lower cellular toxicity than PTMD. Further biological evaluations have to be performed to investigate whether these cell culture results might be confirmed in DM1 models *in vivo*.

## Conclusions

Several studies have demonstrated that certain molecules could partially reverse DM1 symptoms by specifically binding the CUG repeat RNA motif and prevent its further effects in the body. In order to screen a large number of compounds, efficient methods are needed, with low sample requirements and prone to automation.

A relatively fast and efficient CE screening method was developed for the identification of new potentially active compounds for DM1 treatment. This method, in conjunction with other *in vitro* and *in vivo* tests, may be used to improve the workflow of ligand screening, saving time, costs, and materials.

An ACE method using a dynamically coated capillary and HEPES buffer at pH 7.4 as background electrolyte was proposed, simulating physiologically relevant experimental conditions. A total of 13 ligands, including antibiotics and other small molecules, were screened. Only three ligands, neomycin, PTMD, and a PTMD analogue, EBAB, exhibited high affinity for the CUG<sub>50</sub> RNA repeat motif. Even though neomycin shows the highest affinity confirming some of the previously published data, EBAB remains the prime drug candidate due to its high affinity for the CUG probe, while maintaining a low cellular toxicity.

Even though ACE experiments fail to offer information regarding the stoichiometry of the binding process, a simple CE method provided relevant data regarding the similarities between PTMD and EBAB in terms of binding ratio (~120 molecules) with the RNA (CUG)<sub>50</sub> probe. Furthermore, the

therapeutic potential of EBAB in DM1 field was proven for the first time by fluorescence microscopy using a cellular model.

In order to clarify the clinical relevance and pinpoint the potential therapeutic value in DM1 of such interactions between high affinity ligands and the CUG repeats, further studies are still required, testing CUG repeats even closer in length (above 50 repeats) with to the ones occurring in the targeted pathology. Nevertheless, other biomolecular investigations, especially the evaluation of the rescue in the mis-splicing of the involved genes, have to be performed to corroborate the therapeutic potential of EBAB in DM1.

**Funding information** The authors are grateful for financial support from the ABMM (Belgium) and “Iuliu Hațieganu” University of Medicine and Pharmacy (Cluj-Napoca, Romania) through the doctoral research project PCD #7690/78/15.04.2016. Ioan Neaga had a co-financing from the University of Mons.

## Compliance with ethical standards

**Conflict of interest** The authors declare that they have no conflicts of interest.

## References

1. Jameson JL. Principles of molecular medicine. Runge MS, Patterson C, editors. Totowa: Humana Press; 2006.
2. Servadio A, Poletti A, Servadio A, Taroni F. Triplet repeat diseases: from basic to clinical aspects. *Brain Res Bull.* 2001;56:159.
3. Machuca-Tzili L, Brook D, Hilton-Jones D. Clinical and molecular aspects of the myotonic dystrophies: a review. *Muscle Nerve.* 2005;32:1–18.
4. Schara U, Schoser BGH. Myotonic dystrophies type 1 and 2: a summary on current aspects. *Semin Pediatr Neurol.* 2006;13:71–9.
5. Ahmad SI. Neurodegenerative diseases. New-York: Landes Bioscience/Springer Science+Business Media, LLC dual imprint / Springer series: Advances in Experimental Medicine and Biology. 2012.
6. Yotova V, Labuda D, Zietkiewicz E, Gehl D, Lovell A, Lefebvre J-F, et al. Anatomy of a founder effect: myotonic dystrophy in Northeastern Quebec. *Hum Genet.* 2005;117:177–87.
7. Turner C, Hilton-Jones D. The myotonic dystrophies: diagnosis and management. *J Neurol Neurosurg Psychiatry.* 2010;81:358–67.
8. Morgenlander JC, Massey JM. Myotonic dystrophy. *Semin Neurol.* 1991.
9. Harley HG, Walsh KV, Rundle S, Brook JD, Sarfarazi M, Koch MC, et al. Localisation of the myotonic dystrophy locus to 19q13.2?19q13.3 and its relationship to twelve polymorphic loci on 19q. *Hum Genet.* 1991;87:73–80.
10. Brook JD, McCurrach ME, Harley HG, Buckler AJ, Church D, Aburatani H, et al. Molecular basis of myotonic dystrophy: expansion of a trinucleotide (CTG) repeat at the 3' end of a transcript encoding a protein kinase family member. *Cell.* 1992;68:799–808.
11. Martorell L, Monckton DG, Sanchez A, Lopez De Munain A, Baiget M. Frequency and stability of the myotonic dystrophy type 1 premutation. *Neurology* 2001;56:328–335.
12. De Antonio M, Dogan C, Hamroun D, Mati M, Zerrouki S, Eymard B, et al. Unravelling the myotonic dystrophy type 1 clinical spectrum: a systematic registry-based study with implications for disease classification. *Rev Neurol (Paris).* 2016;172:572–80.

13. Gharehbaghi-schnell E, Finsterer J, Korschineck I, Mamoli B. Genotype-phenotype correlation in myotonic dystrophy. *Clin Genet.* 1998;53:20–6.
14. Hamshere MG, Harley H, Harper P, Brook JD, Brookfield JF. Myotonic dystrophy: the correlation of (CTG) repeat length in leucocytes with age at onset is significant only for patients with small expansions. *J Med Genet.* 1999;36:59–61.
15. Schoser B, Timchenko L. Myotonic dystrophies 1 and 2: complex diseases with complex mechanisms. *Curr Genomics.* 2010;11:77–90.
16. Meyers RA. Encyclopedia of molecular cell biology and molecular medicine. *Mol Cell.* 2005;
17. Ho TH. Transgenic mice expressing CUG-BP1 reproduce splicing mis-regulation observed in myotonic dystrophy. *Hum Mol Genet.* 2005;14:1539–47.
18. Coonrod LA, Nakamori M, Wang W, Carrell S, Hilton CL, Bodner MJ, et al. Reducing levels of toxic RNA with small molecules. *ACS Chem Biol.* 2013;8:2528–37.
19. Jasinska A, Michlewski G, de Mezer M, Sobczak K, Kozlowski P, Napierala M, et al. Structures of trinucleotide repeats in human transcripts and their functional implications. *Nucleic Acids Res.* 2003;31:5463–8.
20. Foff EP, Mahadevan MS. Therapeutics development in myotonic dystrophy type 1. *Muscle Nerve.* 2011;44:160–9.
21. Konieczny P, Selma-Soriano E, Rapisarda AS, Fernandez-Costa JM, Perez-Alonso M, Artero R. Myotonic dystrophy: candidate small molecule therapeutics. *Drug Discov Today Elsevier Ltd.* 2017;22:1740–8.
22. van Agtmaal EL, André LM, Willemse M, Cumming SA, van Kessel IDG, van den Broek WJAA, et al. CRISPR/Cas9-induced (CTG-CAG)<sub>n</sub> repeat instability in the myotonic dystrophy type 1 locus: implications for therapeutic genome editing. *Mol Ther Elsevier Ltd.* 2017;25:24–43.
23. Rzuczek SG, Colgan LA, Nakai Y, Cameron MD, Furling D, Yasuda R, et al. Precise small-molecule recognition of a toxic CUG RNA repeat expansion. *Nat Chem Biol.* 2016;13:188–93.
24. Childs-Disney JL, Hoskins J, Rzuczek SG, Thornton CA, Disney MD. Rationally designed small molecules targeting the RNA that causes myotonic dystrophy type 1 are potently bioactive. *ACS Chem Biol.* 2012;7:856–62.
25. García-López A, Llamusi B, Orzáez M, Pérez-Payá E, Artero RD. In vivo discovery of a peptide that prevents CUG-RNA hairpin formation and reverses RNA toxicity in myotonic dystrophy models. *Proc Natl Acad Sci U S A.* 2011;108:11866–71.
26. Nguyen L, Luu LM, Peng S, Serrano JF, Chan HYE, Zimmerman SC. Rationally designed small molecules that target both the DNA and RNA causing myotonic dystrophy type 1. *J Am Chem Soc.* 2015;137:14180–9.
27. Arambula JF, Ramisetty SR, Baranger AM, Zimmerman SC. A simple ligand that selectively targets CUG trinucleotide repeats and inhibits MBNL protein binding. *Proc Natl Acad Sci U S A.* 2009;106:16068–73.
28. Parkesh R, Childs-Disney JL, Nakamori M, Kumar A, Wang E, Wang T, et al. Design of a bioactive small molecule that targets the myotonic dystrophy type 1 RNA via an RNA motif–ligand database and chemical similarity searching. *J Am Chem Soc.* 2012;134:4731–42.
29. Warf MB, Nakamori M, Matthys CM, Thornton CA, Berglund JA. Pentamidine reverses the splicing defects associated with myotonic dystrophy. *Proc Natl Acad Sci U S A.* 2009;106:18551–6.
30. Jahromi AH, Nguyen L, Fu Y, Miller K a, Baranger AM, Zimmerman SC. A novel CUGexp-MBNL1 inhibitor with therapeutic potential for myotonic dystrophy type 1. *ACS Chem Biol.* 2013;8:1037–43.
31. Jahromi AH, Honda M, Zimmerman SC, Spies M. Single-molecule study of the CUG repeat-MBNL1 interaction and its inhibition by small molecules. *Nucleic Acids Res.* 2013;41:6687–97.
32. Wheeler TM, Leger AJ, Pandey SK, MacLeod AR, Nakamori M, Cheng SH, et al. Targeting nuclear RNA for in vivo correction of myotonic dystrophy. *Nature.* 2012;488:111–5.
33. Mulders SAM, van den Broek WJAA, Wheeler TM, Croes HJE, van Kuik-Romeijn P, de Kimpe SJ, et al. Triplet-repeat oligonucleotide-mediated reversal of RNA toxicity in myotonic dystrophy. *Proc Natl Acad Sci.* 2009;106:13915–20.
34. Britz-McKibbin P, Chen DDY. Accurately describing weak analyte-additive interactions by capillary electrophoresis. *Electrophoresis.* 2002;23:880–8.
35. Yang W-C, Yu X-D, Yu A-M, Chen H-Y. Study of a novel cationic calix[4]arene used as selectivity modifier in capillary electrophoresis with electrochemical detection. *J Chromatogr A.* 2001;910:311–8.
36. Hu S, Li PCH. A capillary zone electrophoretic method for the study of formation of a covalent conjugate between microcystin LR and protein phosphatase 2A. *Analyst.* 2001;126:1001–4.
37. Wan Q-H, Le XC. Capillary electrophoretic immunoassays for digoxin and gentamicin with laser-induced fluorescence polarization detection. *J Chromatogr B Biomed Sci Appl.* 1999;734:31–8.
38. Hong M, Cassely A, Mechref Y, Novotny MV. Sugar–lectin interactions investigated through affinity capillary electrophoresis. *J Chromatogr B Biomed Sci Appl.* 2001;752:207–16.
39. Hattori T, Hallberg R, Dubin PL. Roles of electrostatic interaction and polymer structure in the binding of  $\beta$ -lactoglobulin to anionic polyelectrolytes: measurement of binding constants by frontal analysis continuous capillary electrophoresis. *Langmuir.* 2000;16:9738–43.
40. Kiessig S, Reissmann J, Rascher C, Küllertz G, Fischer A, Thünecke F. Application of a green fluorescent fusion protein to study protein-protein interactions by electrophoretic methods. *Electrophoresis.* 2001;22:1428–35.
41. Chen Y-H, Xiao Y, Wu W, Wang Q, Luo G, Dierich MP. HIV-2 transmembrane protein gp36 binds to the putative cellular receptor proteins P45 and P62. *Immunobiology.* 2000;201:317–22.
42. Shimura K, Kasai K-I. Affinity probe capillary electrophoresis of insulin using a fluorescence-labeled recombinant Fab as an affinity probe. *Electrophoresis.* 2014;35:840–5.
43. Zhang L-W, Wang K, Zhang X-X. Study of the interactions between fluoroquinolones and human serum albumin by affinity capillary electrophoresis and fluorescence method. *Anal Chim Acta.* 2007;603:101–10.
44. Zavaleta J, Chinchilla D, Brown A, Ramirez A, Calderon V, Sogomonyan T, et al. Recent developments in affinity capillary electrophoresis: a review. *Curr Anal Chem.* 2006;2:35–42.
45. Michalcová L, Glatz Z. Study on the interactions of sulfonylurea antidiabetic drugs with normal and glycosylated human serum albumin by capillary electrophoresis-frontal analysis. *J Sep Sci.* 2016;39:3631–7.
46. Gonciarz A, Kus K, Szafarz M, Walczak M, Zakrzewska A, Szymura-Oleksiak J. Capillary electrophoresis/frontal analysis versus equilibrium dialysis in dexamethasone sodium phosphate-serum albumin binding studies. *Electrophoresis.* 2012;33:3323–30.
47. Neaga IO, Bodoki E, Hambye S, Blankert B, Oprean R. Study of nucleic acid–ligand interactions by capillary electrophoretic techniques: a review. *Talanta Elsevier.* 2016;148:247–56.
48. Avila LZ, Chu YH, Blossey EC, Whitesides GM. Use of affinity capillary electrophoresis to determine kinetic and equilibrium constants for binding of arylsulfonamides to bovine carbonic anhydrase. *J Med Chem.* 1993;36:126–33.
49. Gomez FA, Avila LZ, Chu Y-H, Whitesides GM. Determination of binding constants of ligands to proteins by affinity capillary electrophoresis: compensation for electroosmotic flow. *Anal Chem.* 1994;66:1785–91.
50. Chu YH, Avila LZ, Biebuyck HA, Whitesides GM. Use of affinity capillary electrophoresis to measure binding constants of ligands to proteins. *J Med Chem.* 1992;35:2915–7.

51. Neubert RH, Ruttinger H-H. Affinity capillary electrophoresis in pharmaceuticals and biopharmaceuticals. 1st ed. Boca Raton: CRC Press; 2003.
52. Michalcová L, Glatz Z. Comparison of various capillary electrophoretic approaches for the study of drug-protein interaction with emphasis on minimal consumption of protein sample and possibility of automation†. *J Sep Sci.* 2015;38:325–31.
53. Swinney K, Bornhop DJ. Detection in capillary electrophoresis. *Electrophoresis.* 2000;21:1239–50.
54. Stanicki D, Pottier M, Gantois N, Pinçon C, Forge D, Mahieu I, et al. Diamidines versus monoamidines as anti-pneumocystis agents: an in vivo study. *Pharmaceuticals.* 2013;6:837–50.
55. Laurent J, Stanicki D, Huang TL, Dei-Cas E, Pottier M, Aliouat EM, et al. Bisbenzamidines as antifungal agents. Are both amidine functions required to observe an anti-pneumocystis carinii activity? *Molecules.* 2010;15:4283–93.
56. Tran NT, Taverna M, Miccoli L, Angulo JF. Poly(ethylene oxide) facilitates the characterization of an affinity between strongly basic proteins with DNA by affinity capillary electrophoresis. *Electrophoresis.* 2005;26:3105–12.
57. Scatchard G. The attractions of proteins for small molecules and ions. *Ann N Y Acad Sci.* 1949;51:660–72.
58. Busch MH, Carels LB, Boelens HF, Kraak JC, Poppe H. Comparison of five methods for the study of drug-protein binding in affinity capillary electrophoresis. *J Chromatogr A.* 1997;777:311–28.
59. McGhee JD, von Hippel PH. Theoretical aspects of DNA-protein interactions: co-operative and non-co-operative binding of large ligands to a one-dimensional homogeneous lattice. *J Mol Biol.* 1974;86:469–89.
60. Rundlett KL, Armstrong DW. Review methods for the estimation of binding constants by capillary electrophoresis. *Electrophoresis.* 1997;18:2194–202.
61. Oravcová J, Böhs B, Lindner W. Drug-protein binding sites. New trends in analytical and experimental methodology. *J Chromatogr B Biomed Appl.* 1996;677:1–28.
62. Bowser MT, Chen DDY. Higher order equilibria and their effect on analyte migration behavior in capillary electrophoresis. *Anal Chem.* 1998;70:3261–70.
63. Colton IJ, Carbeck JD, Rao J, Whitesides GM. Affinity capillary electrophoresis: a physical-organic tool for studying interactions in biomolecular recognition. *Electrophoresis.* 1998;19:367–82.
64. Chen Z, Weber SG. Determination of binding constants by affinity capillary electrophoresis, electrospray ionization mass spectrometry and phase-distribution methods. *Trends Analyt Chem.* 2008;27:738–48.
65. Vamecq J, Maurois P, Pages N, Bac P, Stables JP, Gressens P, et al. 1,2-Ethane bis-1-amino-4-benzamidine is active against several brain insult and seizure challenges through anti-NMDA mechanisms targeting the 3H-TCP binding site and antioxidant action. *Eur J Med Chem.* 2010;45:3101–10.
66. Hambÿe S, Stanicki D, Colet J-M, Aliouat EM, Vanden Eynde JJ, Blankert B. Three optimized and validated (using accuracy profiles) LC methods for the determination of pentamidine and new analogs in rat plasma. *Talanta.* 2011;83:832–9.
67. Hambÿe S, Helvenstein M, Verdy L, Kahvecioglu Z, Conotte R, Vanden Eynde J-J, et al. Ultra high performance liquid chromatography method for the determination of pentamidine and analog in rat biological fluids. *J Pharm Biomed Anal.* 2014;95:54–60.